1

Cardiac Arrhythmias: Mechanistic Knowledge and Innovation from Computer Models

Natalia A. Trayanova and Patrick M. Boyle

Abstract Computational simulation is increasingly recognized as an integral aspect of modern cardiovascular research. Realistic and biophysically detailed models of the cardio-circulatory system can help interpret complex experimental observations, dissect underlying mechanisms, and explain emerging organ-scale phenomena resulting from subtle changes at the tissue, cellular, and/or sub-cellular scales. This chapter provides an overview of recent advances in the simulation of cardiac electrical behavior, focusing specifically on detailed models of the initiation, perpetuation, and termination of ventricular arrhythmias, including fibrillation. The development and validation of such models has opened several noteworthy avenues of research, including close scrutiny of arrhythmia dynamics in healthy and diseased hearts, dissection of arrhythmogenic and cardioprotective properties of specialized cardiac tissue regions such as the Purkinje system, and exploration of emerging paradigms for anti-arrhythmia treatment, such as optogenetics. Excitingly, the clinical community is currently taking the first steps towards using patient-specific ventricular models to stratify arrhythmia risk, personalize treatment planning, and optimize device placement for difficult or unusual procedures.

1.1 Introduction

Computer modeling has emerged as a powerful platform for the investigation of lethal heart rhythm disorders. Biophysically detailed simulations can clarify experimental observations and help reveal how organ-scale arrhythmogenic phenomena (ectopic heartbeats, conduction failure, electrical turbulence, etc.) emerge from pathological effects at the tissue, cell, and protein levels. The development of this ex-

N.A. Trayanova (✉) · P.M. Boyle
Institute for Computational Medicine, Johns Hopkins University, 3400 N Charles St, 316 Hackerman Hall, Baltimore MD 21218, USA
e-mail: ntrayanova@jhu.edu; pmjboyle@jhu.edu

A. Quarteroni (ed.), *Modeling the Heart and the Circulatory System*,
MS&A 14, DOI 10.1007/978-3-319-05230-4_1

tensive "virtual heart" methodology [88, 119, 126, 132] builds upon a strong foundation of research that seeks to use experiments and simulation to quantitatively characterize the action potential response of cardiac cells to electrical stimuli. Simulated action potentials arise from the solution of coupled ordinary differential equation (ODE) systems that model transmembrane current flow through ion channels, pumps, and exchangers as well as the movement of calcium ions between sub-cellular domains. The governing equation for transmembrane current (I_m) is:

$$I_m = C_m \frac{\partial V_m}{\partial t} + I_{ion}, \tag{1.1}$$

where C_m is the membrane capacitance, V_m is the potential difference between the intracellular and extracellular spaces, and I_{ion} is the sum of all ionic currents through membrane channels, pumps, and exchangers. Individual terms added to I_{ion} are also governed by differential equations; for example, the classical description of the fast sodium current (I_{Na}) is:

$$I_{Na} = \overline{g}_{Na} m^3 h \left(V_m - E_{Na}\right), \tag{1.2}$$

where $\overline{g}_{Na}$ is the maximal conductance (based on single channel conductance and overall expression levels), m and h are gating variables defining channel kinetics, and E_{Na} is the reversal potential for sodium ions. The ODE for m is:

$$\frac{\partial m}{\partial t} = \alpha_m (1-m) - \beta_m m = \left[\frac{0.1\,(25 - V_m)}{e^{0.1(25-V_m)} - 1}\right](1-m) - \left[4e^{-\frac{V_m}{18}}\right] m, \tag{1.3}$$

where α_m and β_m are forward and reverse rate constants, respectively. Other gating variables, for I_{Na} and other I_{ion} components, are governed by equations of similar form with parameters tuned to match experimentally observed behavior.

More recently, cardiac modeling has also progressed to the level of the tissue and the whole heart, where the propagation of a wave of action potentials is simulated by a reaction–diffusion partial differential equation (PDE):

$$\nabla \cdot \overline{\sigma}_m \nabla V_m = \beta I_m, \tag{1.4}$$

where $\overline{\sigma}_m$ is the tissue conductivity tensor and β is the myocyte surface area-to-volume ratio. This PDE, known as the monodomain formulation, describes current flow through tissue composed of myocytes that are electrically connected via low-resistance gap junctions. Cardiac tissue has orthotropic electrical conductivities that arise from the cellular organization of the myocardium (cardiac muscle) into fibers and laminar sheets. Global conductivity values are obtained by combining fiber and sheet organization with myocyte-specific local conductivity values. Current flow in the tissue is driven by ionic exchanges across cell membranes during the myocyte action potential. Simultaneous solution of the PDE with the set of action potential ODEs over the tissue volume represents simulation of electrical wave propagation in the myocardium. In certain cases, such as when external current delivery to the

myocardium is simulated, a system of coupled PDEs is used:

$$\nabla \cdot (\overline{\sigma}_i + \overline{\sigma}_e) \nabla \phi_e = -\nabla \cdot \overline{\sigma}_i \nabla V_m - I_e \tag{1.5}$$

$$\nabla \cdot \overline{\sigma}_i \nabla V_m = -\nabla \cdot \overline{\sigma}_i \nabla \phi_e + \beta I_m, \tag{1.6}$$

where $\overline{\sigma}_i$ and $\overline{\sigma}_e$ are the intracellular and extracellular conductivity tensors, ϕ_e is the extracellular potential, and I_e is the current density of extracellular stimulus. This pair of PDEs, known as the bidomain formulation, allows for the explicit representation of current flow in the interstitial (extracellular) space outside cells. Readers interested in a more detailed discussion of the underlying mathematics of cardiac simulations are advised to consult the excellent introductory textbook on bioelectricity by Plonsey and Barr as a starting point [93].

As documented in reviews by Fink et al. [52] and Roberts et al. [101], recent advancements in single-cell action potential modeling have produced building blocks for constructing models of the atria [43, 56, 89], the ventricles [53, 57, 91, 121] and the cardiac conduction system [13, 71, 108, 112, 124] with unprecedented levels of biophysical detail and accuracy. Such developments have helped to fuel the exciting progress made in simulating cardiac electrical behavior at the organ level, which this review is devoted to chronicling. In general, many of the emergent, integrative behaviors in the heart result not only from complex interactions within a specific level but also from feed-forward and feedback interactions that connect a broad range of hierarchical levels of biological organization. The ability to construct multi-scale models of the electrical functioning of the heart, representing integrative behavior from the molecule to the entire organ, is of particular significance since it paves the way for clinical applications of cardiac organ modeling. The review below, while not exhaustive, focuses on both achievements in mechanistic understanding of heart function and dysfunction, and on the trends in the computational medicine aspect of biophysically detailed cardiac modeling applications.

1.2 Basic Cardiac Electrophysiology under Normal and Arrhythmic Conditions

The conduction pathways that underlie normal ventricular activation are shown schematically in Fig. 1.1. During a typical heartbeat (a sequence of events often referred to as normal sinus rhythm), excitation originates spontaneously from a specialized tissue region in the right atrium called the sinoatrial node (SAN). Activation then propagates through the atria to the atrioventricular node (AVN), which is normally the only electrical link between the heart's upper and lower chambers. Excitation then enters the His Bundle (HB), which penetrates into the ventricular septum and divides into the Tawara branches, also called the left and right bundle branches; activation then spreads through the Purkinje system (PS), a topologically complex branching network of fast-conducting fibers that are electrically isolated from underlying myocytes except at endpoints, known as Purkinje-myocardial junctions (PMJs). Finally, coordinated activation of the working ventricular myocardium

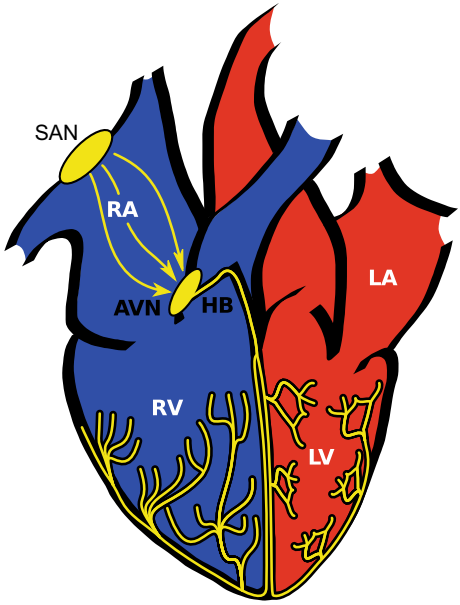

Fig. 1.1. Schematic illustration of cardiac structures involved in normal electrical activation during a heartbeat. The right atrium and ventricle (RA and RV; blue), left atrium and ventricle (LA and LV; red), and specialized conduction system (yellow) are highlighted. In a typical heartbeat, electrical activity initiates spontaneously in the sinoatrial node (SAN) then propagates through the RA to the atrioventricular node (AVN); excitation then spreads into the His bundle (HB) and then the Purkinje system (branching network in LV and RV), which is electrically isolated from ventricular myocardium except at its endpoints. Modified with permission from [30]

is initiated by the emergence of excitatory wavefronts from the spatially distributed PMJ network, which covers a large part of the endocardial surface.

Under certain conditions, normal sinus rhythm can be interfered with or completely subverted by aberrant sources of activation. This state, known as arrhythmia, can be driven by spontaneous ectopic excitations originating from deranged tissue outside the SAN or by reentrant activations, which are periodic self-sustaining waves that rotate around organizing centers. Readers interested in a comprehensive review of concepts and terminology related to reentrant sources and an extensive discussion of implications for cardiac arrhythmia dynamics should consult the excellent review recently published by Pandit and Jalife [92].

1.3 Simulation of Cardiac Arrhythmia

1.3.1 Pro-Arrhythmic Effects of the Cardiac Conduction System

The PS plays a critical role in the coordination of ventricular excitation but it has also been implicated as a key player in arrhythmia initiation and maintenance [36, 44, 45, 102]. Unfortunately, detailed analysis of PS contributions is difficult because its spatiotemporal excitation sequence in the intact heart must be inferred from low-amplitude electrograms [102]. Moreover, chemical ablation of the PS to isolate arrhythmogenic mechanisms is non-selective, since it also destroys several layers of endocardial cells [37]. Circumventing these limitations, computational modeling has provided important insights on arrhythmias involving the PS that would be impossible to achieve otherwise [14,32,33]. For example, ectopic activations from the PS are known to drive catecholaminergic polymorphic ventricular tachycardia (CPVT) [36] but exact organ-scale mechanisms are unknown; Baher et al. [14] proposed an explanation using a 2D ventricular slice model including a representation of the PS. Their study showed that simulation of reciprocating delayed afterpolarization-induced ectopic activations from the left and right sides of the PS gave rise to a bidirectional ECG pattern consistent with CPVT. Another recent study [32] used models of the ventricles with and without the PS to clarify whether elevated endocardial activation rates observed during ventricular fibrillation (VF) were due to activity from nearby PS terminals. Simulations revealed that although PS effects increased the local complexity of VF, transmural rate heterogeneity was most likely caused instead by locally increased expression of ATP-sensitive potassium channels. Finally, in arrhythmias where the PS is a critical part of the reentrant pathway, simulations can be used to guide improvements in clinical diagnosis and treatment. In some patients, the existence of an accessory pathway (AcP) – an abnormal conductive pathway between the atria and ventricles – creates a substrate for macroreentrant supraventricular arrhythmia. Boyle et al. [33] used models with and without AcPs to identify optimal sites for overdrive pacing, a technique used to distinguish AcP-mediated arrhythmia from other tachyardias [125]. As shown in Fig. 1.2, the diagnostic value of this maneuver was greatly improved by pacing near the suspected AcP and far from PS endpoints. For the case where the ventricles were paced from a site near the PS (Fig. 1.2b), the QRS complexes with AcP (left) and without (right) were indistinguishable; in contrast, for second case (Fig. 1.2c), where the pacing site was located far from PS terminals, the "fused" QRS complex from the simulation with the AcP (left) was visibly different from the purely paced case (right). These studies demonstrate how computer modeling can bypass limitations of in vitro experiments to provide mechanistic insights on arrhythmias involving the PS.

Thus far, arrhythmia contributions have only been studied with simple branching network models of the PS, such as those described above [14, 32, 33]; these models adequately simulate the macroscopic functional role of the specialized tissue but lack geometric complexity. In dissected hearts, PS fibers on the endocardium form a distinct network but 3D imaging of these structures remains difficult [109]; as such, another recent research trajectory has focused on the generation of anatomically re-

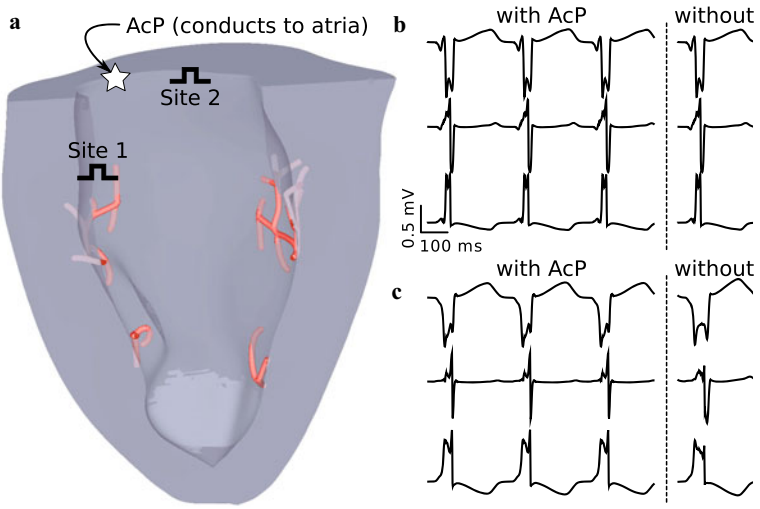

Fig. 1.2. (a) Model of the rabbit ventricles (blue) and Purkinje system (PS; red) with two possible ventricular overdrive pacing sites for diagnosis of supraventricular tachycardia, possibly involving an accessory pathway (AcP) between the atria and the ventricles; (b) and (c) Pseudo-ECG recordings (leads I, II, and III) during overdrive pacing from sites 1 and 2, respectively; sites closer to the PS (e.g., site 1) are a poor choice in terms of diagnostic quality because they fail to produce distinct ("fused") QRS complexes in simulations with (left) versus without (right) the accessory pathway. Modified with permission from [33]

alistic PS models that mimic the physiological network, which could provide insight on how interactions of myocardial tissue with the conduction system affect ventricular arrhythmia dynamics. Ijiri et al. used fractal growth patterns to generate networks that qualitatively resembled the physiological PS [61]. Other groups have adapted this technique [28, 109] to construct patient-specific PS models and explore how PS network complexity affects sinus activation sequence. It will be interesting to see what new insights on PS-mediated arrhythmia dynamics can be gained from simulations that incorporate PS models with increased geometric complexity, which are now a possibility.

1.3.2 Mechanisms Underlying Turbulent Dynamics of Cardiac Arrhythmia

Simulation studies of ventricular electrophysiology have made major contributions to understanding the onset of alternans and the dynamics of VF, the most lethal of all arrhythmias. Particularly interesting are the studies on human hearts [114], which revealed that human VF is driven by a small number of reentrant sources, and is thus much more organized than VF in animal hearts of comparable size; the human action potential duration (APD) was found to be responsible for the specific VF dynamics in the human heart. Electrical alternans, which is beat-to-beat varia-

tion in APD, has long been recognized as a precursor to the development of VF. Alternans can be concordant, with the entire tissue experiencing the same phase of oscillation, or discordant, with opposite-phase regions distributed throughout the tissue. The APD restitution curve slope has been viewed as a major factor both in the onset of arrhythmias following the development of discordant alternans and in the dynamic destabilization of reentrant waves leading to the transition of VT into VF. In what has become known as the restitution hypothesis, flattening the APD restitution curve is postulated to inhibit alternans development and subsequent conduction block, and prevent the onset of VF [54]. Simulation studies employing ventricular models [41, 68, 69] have made important contributions to ascertaining the intricate set of mechanisms by and the conditions under which steep APD restitution could lead to VF onset. These include, but are not limited to, the role of electrotonic and memory effects in suppressing alternans and stabilizing reentrant waves, and the effect of heterogeneous restitution properties on human VF.

Wavefront breakup due to steep APD restitution is not the only possible cause of electrical turbulence seen in VF; Alonso et al. recently showed that in a ventricular model with modestly reduced excitability and APD, the organizing centers (filaments) around which scroll waves rotate tend to increase in length, a phenomenon called "negative tension" [4]. As first characterized in geometrically simple 3D models [5,51], negative tension destabilizes scroll waves, causing increased vorticity and leading to degradation from orderly, VT-like arrhythmias into chaotic VF. Better understanding of negative filament tension could explain situations where VF can be induced despite flat APD restitution.

1.3.3 Mediation of Arrhythmia Dynamics by Mechanically-sensitive Ionic Currents

One of the most important mechanisms of mechanoelectric coupling in the heart is the existence of sarcolemmal channels that are activated by mechanical stimuli. Of these, stretch-activated channels (SACs) have long been implicated as important contributors to the pro-arrhythmic substrate in the heart. However, uncovering the mechanisms by which SACs contribute to ventricular arrhythmogenesis is hampered by the lack of experimental methodologies that can record the 3D electrical and mechanical activity simultaneously and with high spatiotemporal resolution. Thus, computer simulations have emerged as a valuable tool to dissect the mechanisms by which SACs contribute to the ventricular arrhythmogenic substrate.

Early whole-heart modeling attempts to address the role of SACs in the initiation and termination of arrhythmia by a mechanical impact to the chest used pseudo-electromechanical models, in which mechanical activity was not represented but its effect on ventricular electrophysiology was, through SAC recruitment [74,75]. True electromechanical models of the ventricles have been recently developed [60, 67], aimed at investigating the effect of mechanoelectric coupling via SACs on ventricular reentrant wave stability. The study by Hu [60] used an MRI-based electromechanical model of the human ventricles to test the hypothesis that SAC recruitment

affects scroll wave stability differently depending on SAC reversal potential and conductance. The study thus provided a mechanistic insight into the change of organization of VF under abnormal stretch.

1.3.4 Virtual Pharmalogical Screening for Arrhythmogenic Drugs

Relating effects of drugs on ion channels beyond the action potential requires virtual tissue or whole heart organ simulation, so that arrhythmia onset, termination and prevention can be explored. Moreno et al. incorporated both state-dependent Markov modeling of drug effects and full integration to the human action potential (AP), human tissue, and finally realistic MRI image-based human heart [84]. This is the first instance of such massive integration across the space and time scales at play. Their study showed that the effects of flecainide and lidocaine on I_{Na} block are globally similar in response to dynamic protocols. However, clinical trials have shown previously that flecainide tended to be pro-arrhythmic at therapeutic doses, while lidocaine was not. Simulation results made clear that neither simple reduction in I_{Na}, nor single cell behavior could explain this paradox. However, at the macroscopic scale, the vulnerable window was greater for flecainide than for lidocaine (especially in heart failure simulations due to shortened diastole) and reentrant arrhythmia in the ventricle persisted; as discovered by examining Markov states, this was due to the relatively slow accumulation of and recovery from use-dependent block with flecainide.

A common approach to testing potential drugs for cardiotoxicity is to measure hERG channel binding affinity, which indicates whether a compound will prolong the QT interval of the ECG by blocking the rapid delayed rectifier potassium current (I_{Kr}). Many recent studies have sought to use computer modeling to overcome limitations of this screening methodology, such as its high rate of false positives and false negatives. Wilhelms et al. [130] used detailed multiscale models of healthy and ischemic hearts to examine the effects of two drugs that both fail the hERG screening test: cisapride, which is pro-arrhythmic, and amiodarone, which is anti-arrhythmic. Simulations revealed the amiodarone is comparatively safe because in addition to QT prolongation (which was seen for both drugs on simulated ECGs) it also flattened APD restitution. This study and others [35, 48, 136] demonstrate the feasibility of predicting specific drug dose effects on the thoracic ECG. It is hoped that this approach will lead to the development of screening systems that will accelerate cardiotoxicity testing by providing improved reliability compared to the present standard.

1.3.5 Modeling Pathological States to Identify Arrhythmogenic Factors

Simulations have also been conducted to understand ventricular arrhythmia mechanisms for a variety of diseases. Models representing acute myocardial ischemia have characterized the substrate for arrhythmogenesis during the delayed phase (also

called phase 1B), 15 to 45 minutes following coronary artery occlusion; phase 1B is characterized by the presence of an inexcitable midmyocardial layer between still-viable endocardial and epicardial layers; the latter are referred to as border zones. One study [64] showed that heterogeneous coupling between the inexcitable layer and the border zones was pro-arrhythmic; in the case of complete decoupling, reentry could not be induced. In subsequent work [65], the same authors showed that critical levels of sub-epicardial potassium elevation, decoupling between layers, and border zone width were necessary to induce reentry during ischemia phase 1B. Jie et al. [63] used a model of the beating rabbit ventricles to gain insight into the role of electromechanical dysfunction in arrhythmogenesis during acute regional ischemia, both in the induction of ventricular premature beats and in their subsequent degeneration into ventricular arrhythmia.

Computer simulations of ventricular ischemia and infarction and the corresponding body surface potentials have also been used to determine how the extent of the ischemic zone is reflected in the 12-lead ECG. Specifically, modeling research has provided insight on how ECG signals are influenced by the size and shape of acute [127] and healed [135] myocardial infarction. Simulations have also been employed to distinguish between diseases that have similar ECG properties but different underlying cause, which can confound diagnosis and treatment. Potse et al. [95] used ventricular models to show that left bundle branch block and diffuse electrical uncoupling, both of which prolong the QRS complex, can be differentiated by examining ECG amplitude.

Uncovering arrhythmia mechanisms in genetically inherited diseases has also benefited significantly from models of ventricular function [2, 46, 59, 134]. Adeniran et al. [2] developed a Markov model of a mutant I_{Kr} channel known to cause short QT syndrome. Whole heart simulations revealed that increased arrhythmia susceptibility was due to a both APD abbreviation caused by the mutation and intrinsic transmural heterogeneity of I_{Kr} channel expression; when combined, these two factors gave rise to arrhythmogenic APD dispersion. Deo et al. [46] characterized an inward rectifier potassium channel (I_{K1}) mutation from an individual with a different type of short QT syndrome. In addition to reproducing the electrocardiographic phenotype, ventricular simulations with the mutant channel showed that slight (20%) I_{Na} reduction dramatically increased arrhythmia inducibility, suggesting that the use of class I anti-arrhythmic drugs must be closely monitored in the patient. Finally, Hoogendijk et al. [59] showed that I_{Na} reduction, which is associated with Brugada syndrome, leads to conduction block due to source-sink mismatch at microscopic tissue heterogeneities; simulations revealed that the severity of this effect is modulated by other Brugada-linked mutations, such as increased transient outward potassium current and decreased L-type calcium current.

1.3.6 Modeling to Identify Individuals with a High Risk of Developing Arrhythmia

Robust methods for stratifying the risk of lethal cardiac arrhythmias decrease morbidity and mortality in patients with cardiovascular disease and reduce health care costs [55]. The most widely used approaches currently used for stratifying cardiac arrhythmia risk involve testing for ECG abnormalities, then using the results to identify patients who would benefit from implantable cardioverter defibrillator (ICD) therapy. However, the mechanisms underlying these ECG indices, and their relationship to lethal arrhythmias, are not fully understood. Computational models of the heart have made inroads in this clinical cardiology arena [17, 18, 38, 47, 66, 85, 90, 137]. Specifically, research has reported a strong correlation between increased arrhythmia risk and the presence of microvolt T-wave alternans (MTWA) [26,58]. However, the mechanistic basis of MTWA preceding lethal ventricular arrhythmias has been under debate since MTWA is most successful in stratifying risk in patients at heart rates < 110 bpm, where APD restitution is flat [86]. Computational models of the left ventricular (LV) wall in combination with clinical data revealed that abnormal intracellular calcium handling underlies alternans in action potential voltage, which result in MTWA at heart rates < 110 bpm [17, 85]; abnormalities in intracellular calcium have long been linked to ventricular fibrillation [80, 129]. Computational modeling studies have also shown that under conditions of abnormal calcium dynamics, the T-wave alternans magnitude is enhanced by structural heterogeneities in the myocardium [47].

Recently, a computational model of the human ventricles was used to demonstrate that detecting instabilities in the QT interval in the clinical ECGs could predict the onset of VT, particularly in patients with acute myocardial infarction [38]. The study explored the effect of frequency of premature activation, which was controlled in the model by shortening the beat-to-beat coupling interval for different numbers of randomly-selected beats in minute-long sinus activation sequences; increased frequency of premature activation was found to precede VT onset by leading to instability in the QT interval. Therefore, screening the QT interval of the ECG for instabilities using the novel algorithm developed by Chen and Trayanova [38, 40] could potentially be a robust risk stratification method for patients with acute myocardial infarction. Recently, the approach was successfully applied to stratify the risk of arrhythmias in 114 patients with ICDs [39]. These studies pave the way for executing computer simulations to determine patient-specific thresholds for arrhythmia stratification ECG indices, rather than relaying on clinical guidelines based on large and diverse patient cohorts. Another approach to arrhythmia risk stratification that has recently gained traction is the use of computer models to predict the arrhythmia outcome in patients that exhibit potentially lethal mutations in genes encoding cardiac proteins associated with long QT syndrome [18, 66, 90, 137]. These studies chart new directions for future genotype-based risk stratification and personalized gene therapy.

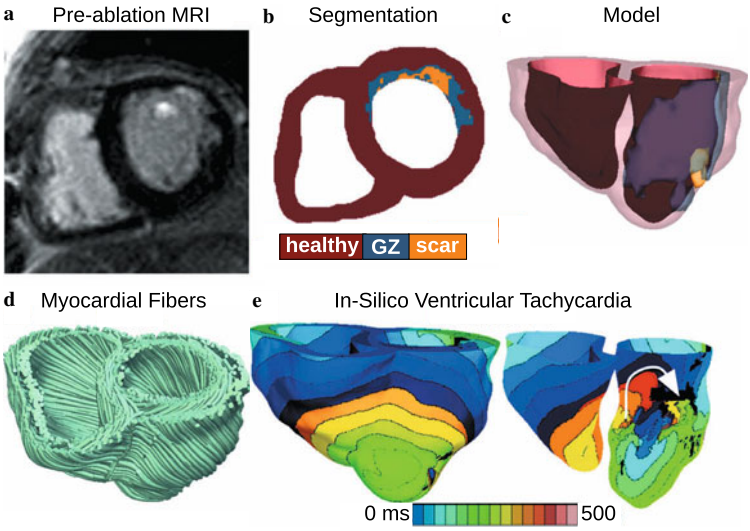

Fig. 1.3. (a) and (b) Clinical MRI scan of an infarcted patient heart and the corresponding segmentation; (c) 3D geometric model of the patient heart with the epicardium and the infarct border zone rendered semi-transparent; (d) Estimated fiber orientations; (e) Simulated activation map of ventricular tachycardia (VT) revealing reentry on the left ventricular endocardium. VT frequency is 3.05 Hz. Color bar indicates activation times. White arrow indicates path of reentrant wave. Modified with permission from [132]

1.3.7 Clinical Applications of Simulation-based Arrhythmia Research

Recent years have witnessed revolutionary advances in imaging, including ex vivo structural and diffusion tensor (DT) magnetic resonance imaging (MRI) that facilitate acquisition of the intact structure of explanted hearts with high resolution. Leveraging these advances, a new generation of whole-heart image-based models with unprecedented detail has emerged [22, 123]. Such models are currently being used, in combination with experimental electrophysiological data, to provide better understanding of the role of the individual infarct region morphology in the generation and maintenance of infarct-related VT, the most frequent clinical ventricular arrhythmia, present in 64% of patients with ventricular rhythm disorder and in 89% of patients with sudden cardiac death [111]. Using a model of the infarcted pig ventricles reconstructed from ex-vivo MRI and DTMRI data, Pop et al. [94] demonstrated good correspondence between in-silico and experimental electroanatomical voltage maps, and successfully predicted infarct-related VT inducibility after programmed electrical stimulation. Arevalo et al. [8] examined the role infarct border zone extent in arrhythmogenesis, establishing that a minimum volume of remodeled tissue is needed for VT maintenance and demonstrating that the organizing center of infarct-related VT is located within the border zone, regardless of the pacing site from which VT

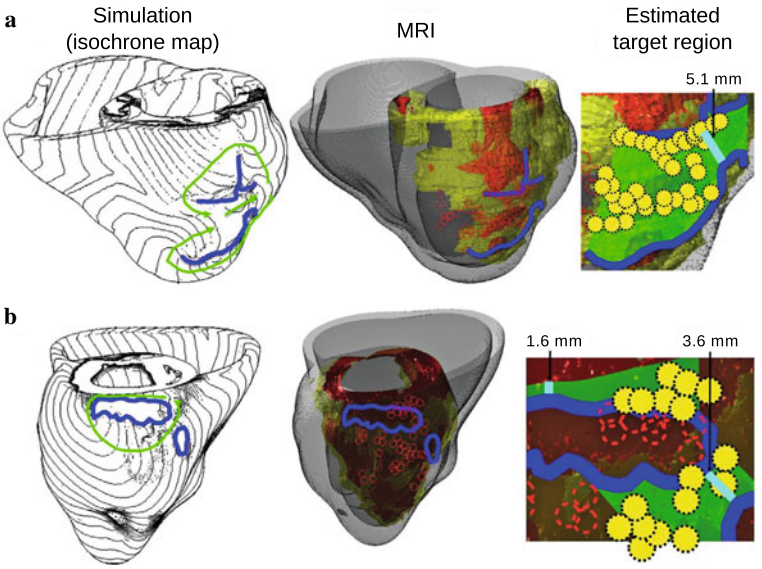

Fig. 1.4. (a) and (b) Comparison between simulation-guided and standard electrophysiological approaches for identifying ablation targets in two patients with infarct-related VTs. Left column: propagation pathways (green) and lines of conduction block (blue) are overlaid over VT activation maps simulated in image-based patient heart models. Middle column: pre-ablation infarct geometry (infarct scar: orange, border zone: yellow, non-infarcted: gray) along with ablation lesions delivered by the standard approach (red circles) and conduction block lines as calculated from ventricular simulations. Right column: optimal ablation zones (green shading) predicted by simulations, with narrowest isthmuses indicated (cyan); in both cases, only a fraction of the ablation sites from the standard approach were within the predicted optimal ablation zone (yellow circles). Modified with permission from [12]

is induced. Such simulation methodology could have a major clinical impact in predicting the optimal targets for catheter ablation of infarct-related VT in individual hearts, should the methodology be able to reconstruct patent hearts from clinical imaging data and evaluate the 3D patterns of infarct-related VT in the patient. The first attempts in this direction have already been made. Figure 1.3 presents a simulation of arrhythmia in a patient-specific model of the infarcted ventricles; it shows model generation from clinical MR scans of the patient heart as well as simulated infarct-related ventricular tachycardia [132]. Figure 1.4, from the recent study by Ashikaga et al., [12] demonstrates that non-invasive simulation prediction of optimal targets for ablation of infarct-related VT could result in lesions that are much smaller than those executed in the clinic.

Several additional studies are noteworthy. Zhu et al. [138] showed that models of the heart can be used to carry out non-invasive localization of accessory pathways in patients with Wolff-Parkinson-White syndrome. Ng et al. [87] demonstrated the feasibility of using simulations to predict VT circuits. Relan et al. [99] used a hy-

brid X-ray and MR environment to image a patient heart, which was further personalized with voltage measurements. The results demonstrated that the heart model could successfully be used to assess infarct-related VT inducibility from sites not accessible in the clinic. Further translation of ventricular simulations in the clinic will be facilitated by the development of methodologies to estimate patient-specific fiber orientations from clinical MRI scans [16, 122].

1.4 Simulation of Cardiac Arrhythmia Termination

Controlling the complex spatio-temporal dynamics underlying life-threatening cardiac arrhythmias such as fibrillation is extremely difficult because of the nonlinear interaction of excitation waves within the heterogeneous anatomical substrate. In the absence of a better strategy, strong electrical shocks have remained the only reliable treatment for cardiac fibrillation. Over the years, biophysically-detailed multi-scale models of defibrillation [3, 6, 105, 107] have made major contributions to understanding how defibrillation shocks used in clinical practice interact with cardiac tissue [7, 9, 11, 29, 50, 78, 103, 104, 115, 118]; these models have been validated by comparing to the results of optimal mapping experiments [20, 24, 25]. Computer modeling of whole-heart defibrillation has been instrumental in the development of the virtual electrode polarization (VEP) theory for defibrillation. Research has found that mechanisms for shock success or failure are multifactorial, depending mainly on the postshock distribution of transmembrane potential as well as the timing and propagation speed of shock-induced wavefronts. Recent simulation studies have been instrumental in understanding mechanisms of the isoelectric window that follows defibrillation shocks with strength near the defibrillation threshold (DFT): one of the proposed explanations for the isoelectric window duration is propagation of postshock activations in intramural excitable areas ("tunnel propagation"), bounded by long-lasting postshock depolarization of the cardiac surfaces [10, 42].

Ventricular simulations have also ascertained the role of cardiac microstructure in the mechanisms of defibrillation. For example, Bishop et al. applied shocks to a very high-resolution ($\sim 25\ \mu m$ voxel size) image-based rabbit ventricular model; VEPs formed at the boundaries between blood vessels and myocardium [19], which gave rise to secondary sources that eliminated excitable gaps and led to successful defibrillation [23]. Simulations have also contributed to understanding of the process of defibrillation in hearts with myocardial ischemia and infarction [96, 105, 106], uncovering the role of electrophysiological and structural remodeling in the failure or success of the shock. Finally, simulations were conducted in a rabbit ventricular electromechanics model to examine vulnerability to strong shocks and defibrillation under the conditions of LV dilation and determine the mechanisms by which mechanical deformation may lead to increased vulnerability and elevated DFT [72, 117, 120]. The results suggested that ventricular geometry and the rearrangement of fiber architecture in the deformed ventricles is responsible for the reduced defibrillation efficacy in the dilated ventricles.

1.4.1 Model-Based Innovation to Improve Arrhythmia Termination by Electric Shocks

Recently, defibrillation modeling has focused on the development of new methodologies for low-voltage termination of lethal arrhythmias or for applying defibrillation in novel, less damaging ways. The study by Tandri et al. [113] used sustained kilohertz-range alternating current (AC) fields for arrhythmia termination. Termination of arrhythmia with AC fields has been attempted previously in simulations [81–83] with limited success; the frequencies used in these studies were, however, substantially lower. The premise of the Tandri et al. study was that such fields have been known to instantaneously and reversibly block electrical conduction in nerve tissue. Aided by ventricular modeling, the article provided proof of the concept that electric fields, such as those used for neural block, when applied to cardiac tissue, similarly produce reversible block of cardiac impulse propagation and lead to successful defibrillation; it also showed that this methodology could potentially be a safer means for terminating life-threatening reentrant arrhythmias. Since the same AC fields block equally well both neural and cardiac activity, the proposed defibrillation methodology could possibly be utilized to achieve high-voltage yet painless defibrillation. The follow-up study by Weinberg et al. [128] provided, again using ventricular simulations, a deeper analysis of the mechanisms that underlie the success and failure of this novel mode of defibrillation.

Recent experimental studies have shown that applied electric fields delivering multiple far-field stimuli at a given cycle length can terminate VT, atrial flutter, and atrial fibrillation with less total energy than a single strong shock [73, 76, 79]. However, the mechanisms and full range of applications of this new mode of defibrillation have remained poorly explored. The recent simulation study by Rantner at al. [97] aimed to elucidate these mechanisms and to develop an optimal low-voltage defibrillation protocol. Based on the simulation results using a complex high-resolution MRI-based ventricular wall model, a novel two-stage low-voltage defibrillation protocol was proposed that did not involve the delivery of the stimuli at a constant cycle length. Instead, the first stage converted VF into VT by applying low-voltage stimuli at instants of maximal excitable gap, capturing large tissue volume and synchronizing depolarization. The second stage was designed to terminate VT, in cases where it persisted, by multiple low-voltage stimuli given at constant cycle lengths. The energy required for successful defibrillation using this protocol was 57.42% of the energy for low-voltage defibrillation when stimulating at the optimal fixed-duration cycle length.

1.4.2 Exploration of an Emerging Paradigm for Anti-arrhythmia Treatment: Cardiac Optogenetics

Cardiac optogenetics is an emerging field that involves inserting light-sensitive ion channels (opsins) in heart tissue to enable control of bioelectric behavior with illumination instead of electric current [49, 131]. This technology is poised to open a new avenue for the development of safe and effective anti-arrhythmia therapies by enabling the evocation of spatiotemporally precise responses in targeted cells or tissues. Abilez et al. [1] conducted ventricular simulations with a Markov model of light-sensitive current incorporated at the cell scale in selected regions; a later study from the same group [133] showed that differences between optically and electrically stimulated cells were limited to mild changes in intracellular sodium and potassium concentrations. Boyle et al. [34] developed a comprehensive whole-heart optogenetics simulation platform that incorporates realistic representations of opsin delivery as well as the response to illumination at the molecular, cell, tissue, and organ scales. This framework was then used to explore how opsin delivery characteristics determine energy requirements for optical stimulation and to identify cardiac structures that are potential pacemaking targets with low optical excitation threshold. As shown in Fig. 1.5, optical stimulation was more efficient when cell-specific optogenetic targeting was used to express opsins in the PS compared to ventricular cells. This finding is particularly noteworthy because direct pacing of the His bundle has therapeutic advantages compared to conventional pacing for cardiac resynchronization [15], but the practical usefulness of this maneuver is limited by high energy requirements and low selectivity (i.e., electrical stimuli capture the ventricular septum as well as the His bundle). Results from optogenetics simulations indicate that both

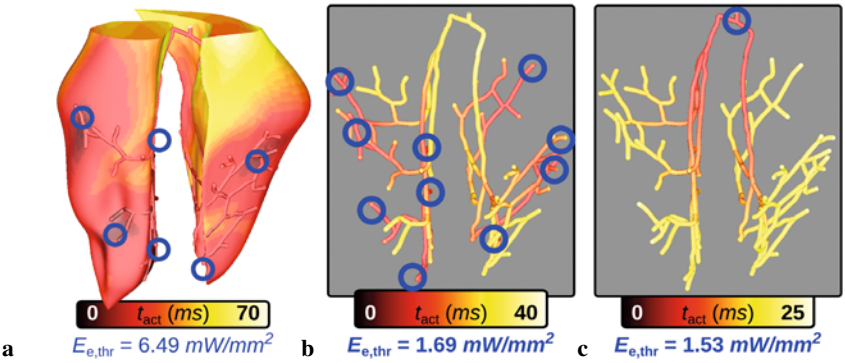

a b c

Fig. 1.5. Activation sequences in response to intracardiac optical stimulation (blue circles) in a model of the rabbit ventricles and PS with simulated optogenetic delivery of light-sensitive ion channels targeted to ventricular cells only (a) or Purkinje system (PS) cells only (b, c). The threshold irradiance ($E_{e,thr}$) to elicit a propagating AP response by illumination was significantly lower in cases where the PS was targeted. All activation times (t_{act}) are measured with respect to the delivery of a 2 ms light pulse at $1.1 \times E_{e,thr}$ to the endocardial surface under each site shown. Modified with permission from [34]

of these shortcomings could be overcome by using a light-based approach for the same type of stimulation. Modeling will provide valuable insights to help guide the development of this type of low-energy solution for managing cardiac arrhythmias.

As summarized in a recent editorial [31], innovative developments in light-sensitive protein engineering [77], intracardiac optics [70], and cardiac gene therapy [27, 62] suggest that such optogenetics-based arrhythmia termination therapies could be a reality in the not-so-distant future. However, the clinical feasibility of these strategies remains largely untested. Simulations conducted in virtual light-sensitized hearts will provide valuable insights to help guide the development of experiments that will lay the groundwork for therapeutic applications of cardiac optogenetics. For example, Boyle et al. reported [31] that simulated gene delivery of the light-sensitive protein channelrhodopsin-2 (ChR2) to a model of the diseased human atria enables cardioversion of arrhythmias by illumination of the endocardial surface.

1.4.3 Leveraging Patient-Specific Models to Optimize Difficult Clinical Procedures

Finally, a recent study [98] has made the first attempt towards clinical translation of computer models of arrhythmia termination. It addressed a clinical need: ICDs with transvenous leads often cannot be implanted in a standard manner in pediatric and congenital heart defect (CHD) patients; currently, there is no reliable approach to predict the optimal ICD placement in these patients. The study provided proof-of-concept that patient-specific, biophysically detailed computer simulations of the dynamic process of defibrillation could be used to predict optimal ICD lead location in these patients. A pipeline for constructing personalized, electrophysiological heart-and-torso models from clinical MRI scans was developed and applied to a pediatric CHD patient, and the optimal ICD placement was determined using patient-specific simulations of defibrillation. In a patient with tricuspid valve atresia, two configurations with epicardial leads were found to have the lowest defibrillation threshold. As shown in Fig. 1.6, the optimal configurations were associated with significantly lower defibrillation thresholds compared to alternative lead/can combinations. The study demonstrated that by using such methodology the optimal ICD placement in pediatric/CHD patients could be predicted computationally, which could reduce defibrillation energy if the pipeline is used as part of ICD implantation planning.

1.5 Computational Complexity of Cardiac Electrophysiology Simulations

Although it would be impractical to provide model details and runtime information for all of the 100+ models cited in this review, we provide here a brief discussion of computational complexity in cardiac simulations, which is an important practical consideration for the field. Many factors contribute to the overall complexity of each individual model, including the type of activity being simulated; the scale

a

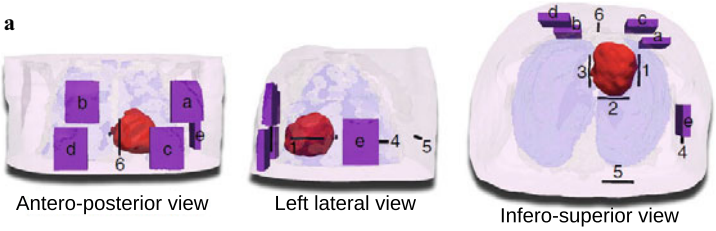

b

Lead Position(s)	Can Position	Rel. DFT
left epicardial (1)	right chest (d)	1
posterior epicardial (2)	left chest (c)	1
right epicardial (3)	sub-clavicular (a)	2
left subcutaneous (4)	right para-sternal (b)	32
left subcutaneous (4)	right chest (d)	16
posterior subcutaneous (5)	sub-clavicular (a)	8
posterior subcutaneous (5)	left chest (c)	8
left para-sternal (6)	sub-axillary (e)	8
left subcutaneous (4) + posterior subcutaneous (5) + left para-sternal (6)	sub-clavicular (a)	8
posterior subcutaneous (5) + left para-sternal (6)	sub-clavicular (a)	64
posterior subcutaneous (5) + left para-sternal (6)	sub-axillary (e)	8

Fig. 1.6. (a) Patient-specific model of heart (red) and torso with skin (pink), lungs (blue), and bones (white); possible locations for the implantable cardioverter defibrillator (ICD) can (purple; a–e) and lead (black; 1-6) are also superimposed; (b) Lead and can positions and relative defibrillation thresholds (DFT) for each of the 11 ICD configurations tested in the study are tabulated. Relative DFT values are calculated with respect to those determined for the first two cases (top lines in table). Modified with permission from [98]

and resolution of the cardiac geometry; and, the size and characteristics of the ODE system representing myocyte membrane kinetics. These factors and their impact on the computational resources required vary dramatically from study to study. Simulations that require application of the bidomain formulation (e.g., defibrillation studies [23, 44, 96, 97, 116]) are more time-consuming than those in which the monodomain formulation is adequate. Mesh size varies dramatically depending on the size of the model and the resolution necessary to capture details relevant to phenomena of interest; this review discusses studies involving models with degrees of freedom (i.e., mesh nodes) ranging from hundreds of thousands [32,33,44,45,104–107] to millions [19,21–23,96–98] and even tens of millions [95]. At the cell level, ionic models that aim to represent different levels of detail vary considerably in terms of the size of the associated ODE system; for example, the Courtemanche human atrial

model has 19 equations [43], the O'Hara human ventricular model has 43 [91], and the Sampson human Purkinje fiber model has 83 [108]. Furthermore, in cases where these ODE systems are stiff (i.e., rate constants associated with individual state variables in the model differ dramatically), computational complexity increases because it becomes necessary to use extremely short time steps or implement higher-order ODE solvers (e.g., Runge-Kutta or Rosenbrock schemes) [110]. Due to these many layers of complexity, biophysically detailed whole heart simulations tend to be extremely time consuming, even when state-of-the-art computing resources are used – one recent review estimated that compute time generally lags real time by 3 to 4 orders of magnitude (i.e., a one-second heart beat takes 1000 to 10000 seconds to simulate) [119]. As of this writing, simulations conducted on the most powerful supercomputer ever used to conduct high-resolution, organ-scale cardiac modeling research still lagged real-time by 12% [100].

1.6 The Future of Computational Cardiac Electrophysiology

As this review demonstrates, the key in attaining predictive capabilities of multi-scale biophysically-detailed cardiac models at the level of the organ has been the use of geometrically realistic (typically MRI- or CT- based) models of the ventricles, and the application of diffusion tensor DT-MRI to measure the anatomy, fiber, and sheet structure of the heart, in cases of ex-vivo studies. This has led to a new generation of image-based ventricular models with unprecedented structural and biophysical detail. Clearly, models of cardiac function have benefited significantly from this revolution in medical imaging.

As outlined above, cardiac models have been used to gain insights into mechanisms of arrhythmia in many disease settings and to understand how external currents can terminate ventricular arrhythmias. In addition, a major thrust in computational cardiac electrophysiology is to use models as a test bed for evaluation of new antiarrhythmic drugs. It is now possible to test hypotheses regarding mechanisms of drug action on the scale of the whole heart. Multi-scale heart models of antiarrhythmic drug interactions with ion channels have provided insights into why certain pharmacological interventions result in pro-arrhythmia, whereas others do not. This work has the potential to more effectively guide the drug development pipeline – a process that currently has high failure rates and high costs.

The use of heart models in personalized diagnosis, treatment planning, and prevention of sudden cardiac death is also slowly becoming a reality, as reviewed here. The feasibility of subject-specific modeling has been demonstrated through the use of heart models reconstructed from clinical MRI scans. Computer simulations of the function of the diseased heart represent a profound example of a research avenue in the new discipline of computational medicine. Biophysically detailed models of the heart assembled with data from clinical imaging modalities that incorporate electrophysiological and structural remodeling in cardiac disease are poised to become a first line of screening for new therapies and approaches, new diagnostic develop-

ments, and new methods for disease prevention. Implementing patient-specific cardiac simulations at the patient bedside could become one of the most thrilling examples of computational science and engineering approaches in translational medicine.

Acknowledgements This research was supported by the following grants: NIH-DP1-HL123271, NIH-R01-HL103428, NIH-R01-HL105216, NIH-R01-HL094610, and NSF-CDI-1124804.

References

1. Abilez, O.J., Wong, J., Prakash, R., Deisseroth, K., Zarins, C.K., Kuhl, E.: Multiscale computational models for optogenetic control of cardiac function. Biophys. J. **101**(6), 1326–34 (2011)
2. Adeniran, I., McPate, M.J., Witchel, H.J., Hancox, J.C., Zhang, H.: Increased vulnerability of human ventricle to re-entrant excitation in herg-linked variant 1 short QT syndrome. PLoS. Comput. Biol. **7**(12), e1002,313 (2011)
3. Aguel, F., Debruin, K.A., Krassowska, W., Trayanova, N.A.: Effects of electroporation on the transmembrane potential distribution in a two-dimensional bidomain model of cardiac tissue. J. Cardiovasc. Electrophysiol. **10**(5), 701–14 (1999)
4. Alonso, S., Bar, M., Panfilov, A.V.: Negative tension of scroll wave filaments and turbulence in three-dimensional excitable media and application in cardiac dynamics. Bull. Math. Biol. **75**(8), 1351–76 (2013)
5. Alonso, S., Panfilov, A.V.: Negative filament tension at high excitability in a model of cardiac tissue. Phys. Rev. Lett. **100**(21), 218,101 (2008)
6. Anderson, C., Trayanova, N., Skouibine, K.: Termination of spiral waves with biphasic shocks: role of virtual electrode polarization. J. Cardiovasc. Electrophysiol. **11**(12), 1386–96 (2000)
7. Anderson, C., Trayanova, N.A.: Success and failure of biphasic shocks: results of bidomain simulations. Math. Biosci. **174**(2), 91–109 (2001)
8. Arevalo, H., Plank, G., Helm, P., Halperin, H., Trayanova, N.: Tachycardia in postinfarction hearts: Insights from 3D image-based ventricular models. PLoS. One. **8**(7), e68,872 (2013)
9. Arevalo, H., Rodriguez, B., Trayanova, N.: Arrhythmogenesis in the heart: Multiscale modeling of the effects of defibrillation shocks and the role of electrophysiological heterogeneity. Chaos **17**(1), 015,103 (2007)
10. Ashihara, T., Constantino, J., Trayanova, N.A.: Tunnel propagation of postshock activations as a hypothesis for fibrillation induction and isoelectric window. Circ. Res. **102**(6), 737–45 (2008)
11. Ashihara, T., Trayanova, N.A.: Asymmetry in membrane responses to electric shocks: insights from bidomain simulations. Biophys. J **87**(4), 2271–82 (2004)
12. Ashikaga, H., Arevalo, H., Vadakkumpadan, F., Blake R. C., Bayer, J.D., Nazarian, S., Muz Zviman, M., Tandri, H., Berger, R.D., Calkins, H., Herzka, D.A., Trayanova, N.A., Halperin, H.R.: Feasibility of image-based simulation to estimate ablation target in human ventricular arrhythmia. Heart Rhythm **10**(8), 1109–16 (2013)
13. Aslanidi, O.V., Sleiman, R.N., Boyett, M.R., Hancox, J.C., Zhang, H.: Ionic mechanisms for electrical heterogeneity between rabbit Purkinje fiber and ventricular cells. Biophys. J. **98**(11), 2420–31 (2010)

14. Baher, A.A., Uy, M., Xie, F., Garfinkel, A., Qu, Z., Weiss, J.N.: Bidirectional ventricular tachycardia: ping pong in the His-Purkinje system. Heart Rhythm **8**(4), 599–605 (2011)
15. Barba-Pichardo, R., Manovel Sanchez, A., Fernandez-Gomez, J.M., Morina-Vazquez, P., Venegas-Gamero, J., Herrera-Carranza, M.: Ventricular resynchronization therapy by direct His-bundle pacing using an internal cardioverter defibrillator. Europace **15**(1), 83–8 (2013)
16. Bayer, J.D., Blake, R.C., Plank, G., Trayanova, N.A.: A novel rule-based algorithm for assigning myocardial fiber orientation to computational heart models. Ann. Biomed. Eng. **40**(10), 2243–54 (2012)
17. Bayer, J.D., Narayan, S.M., Lalani, G.G., Trayanova, N.A.: Rate-dependent action potential alternans in human heart failure implicates abnormal intracellular calcium handling. Heart Rhythm **7**(8), 1093–101 (2010)
18. Benson, A.P., Al-Owais, M., Holden, A.V.: Quantitative prediction of the arrhythmogenic effects of de novo hERG mutations in computational models of human ventricular tissues. Eur. Biophys. J **40**(5), 627–39 (2011)
19. Bishop, M.J., Boyle, P.M., Plank, G., Welsh, D.G., Vigmond, E.J.: Modeling the role of the coronary vasculature during external field stimulation. IEEE Trans. Biomed. Eng. **57**(10), 2335–45 (2010)
20. Bishop, M.J., Gavaghan, D.J., Trayanova, N.A., Rodriguez, B.: Photon scattering effects in optical mapping of propagation and arrhythmogenesis in the heart. J. Electrocardiol. **40**(6 Suppl.), S75–80 (2007)
21. Bishop, M.J., Plank, G.: The role of fine-scale anatomical structure in the dynamics of reentry in computational models of the rabbit ventricles. J. Physiol. **590**(Pt 18), 4515–35 (2012)
22. Bishop, M.J., Plank, G., Burton, R.A., Schneider, J.E., Gavaghan, D.J., Grau, V., Kohl, P.: Development of an anatomically detailed MRI-derived rabbit ventricular model and assessment of its impact on simulations of electrophysiological function. Am. J. Physiol. Heart Circ. Physiol. **298**(2), H699–718 (2010)
23. Bishop, M.J., Plank, G., Vigmond, E.: Investigating the role of the coronary vasculature in the mechanisms of defibrillation. Circ Arrhythm Electrophysiol **5**(1), 210–9 (2012)
24. Bishop, M.J., Rodriguez, B., Eason, J., Whiteley, J.P., Trayanova, N., Gavaghan, D.J.: Synthesis of voltage-sensitive optical signals: application to panoramic optical mapping. Biophys. J. **90**(8), 2938–45 (2006)
25. Bishop, M.J., Rodriguez, B., Qu, F., Efimov, I.R., Gavaghan, D.J., Trayanova, N.A.: The role of photon scattering in optical signal distortion during arrhythmia and defibrillation. Biophys. J **93**(10), 3714–26 (2007)
26. Bloomfield, D.M., Bigger, J.T., Steinman, R.C., Namerow, P.B., Parides, M.K., Curtis, A.B., Kaufman, E.S., Davidenko, J.M., Shinn, T.S., Fontaine, J.M.: Microvolt t-wave alternans and the risk of death or sustained ventricular arrhythmias in patients with left ventricular dysfunction. J. Am. Coll. Cardiol. **47**(2), 456–63 (2006)
27. Bolli, R., Chugh, A.R., D'Amario, D., Loughran, J.H., Stoddard, M.F., Ikram, S., Beache, G.M., Wagner, S.G., Leri, A., Hosoda, T., Sanada, F., Elmore, J.B., Goichberg, P., Cappetta, D., Solankhi, N.K., Fahsah, I., Rokosh, D.G., Slaughter, M.S., Kajstura, J., Anversa, P.: Cardiac stem cells in patients with ischaemic cardiomyopathy (SCIPIO): initial results of a randomised phase 1 trial. Lancet **378**(9806), 1847–57 (2011)
28. Bordas, R., Gillow, K., Lou, Q., Efimov, I.R., Gavaghan, D., Kohl, P., Grau, V., Rodriguez, B.: Rabbit-specific ventricular model of cardiac electrophysiological function including specialized conduction system. Prog. Biophys. Mol. Biol. **107**(1), 90–100 (2011)

29. Bourn, D.W., Gray, R.A., Trayanova, N.A.: Characterization of the relationship between preshock state and virtual electrode polarization-induced propagated graded responses resulting in arrhythmia induction. Heart Rhythm **3**(5), 583–95 (2006)
30. Boyle, P.M.: Roles of the Purkinje system during electric shocks and arrhythmia. Doctoral dissertation, University of Calgary (2011)
31. Boyle, P.M., Entcheva, E., Trayanova, N.A.: See the light: can optogenetics restore healthy heartbeats? and, if it can, is it really worth the effort? Expert Review of Cardiovascular Therapy **12**(1), 1–4 (2014)
32. Boyle, P.M., Masse, S., Nanthakumar, K., Vigmond, E.J.: Transmural IK(ATP) heterogeneity as a determinant of activation rate gradient during early ventricular fibrillation: Mechanistic insights from rabbit ventricular models. Heart Rhythm **10**, 1710–7 (2013)
33. Boyle, P.M., Veenhuyzen, G.D., Vigmond, E.J.: Fusion during entrainment of orthodromic reciprocating tachycardia is enhanced for basal pacing sites but diminished when pacing near Purkinje system end points. Heart Rhythm **10**(3), 444–51 (2013)
34. Boyle, P.M., Williams, J.C., Ambrosi, C.M., Entcheva, E., Trayanova, N.A.: A comprehensive multiscale framework for simulating optogenetics in the heart. Nat. Commun. **4**, 2370 (2013)
35. Carusi, A., Burrage, K., Rodriguez, B.: Bridging experiments, models and simulations: an integrative approach to validation in computational cardiac electrophysiology. Am. J. Physiol. Heart Circ. Physiol. **303**(2), H144–55 (2012)
36. Cerrone, M., Noujaim, S.F., Tolkacheva, E.G., Talkachou, A., O'Connell, R., Berenfeld, O., Anumonwo, J., Pandit, S.V., Vikstrom, K., Napolitano, C., Priori, S.G., Jalife, J.: Arrhythmogenic mechanisms in a mouse model of catecholaminergic polymorphic ventricular tachycardia. Circ. Res. **101**(10), 1039–48 (2007)
37. Cha, Y.M., Uchida, T., Wolf, P.L., Peters, B.B., Fishbein, M.C., Karagueuzian, H.S., Chen, P.S.: Effects of chemical subendocardial ablation on activation rate gradient during ventricular fibrillation. Am. J. Physiol. **269**(6 Pt 2), H1998–2009 (1995)
38. Chen, X., Hu, Y., Fetics, B.J., Berger, R.D., Trayanova, N.A.: Unstable QT interval dynamics precedes ventricular tachycardia onset in patients with acute myocardial infarction: a novel approach to detect instability in qt interval dynamics from clinical ECG. Circ. Arrhythm. Electrophysiol. **4**(6), 858–66 (2011)
39. Chen, X., Tereshchenko, L.G., Berger, R.D., Trayanova, N.A.: Arrhythmia risk stratification based on QT interval instability: an intracardiac electrocardiogram study. Heart Rhythm **10**(6), 875–80 (2013)
40. Chen, X., Trayanova, N.A.: A novel methodology for assessing the bounded-input bounded-output instability in qt interval dynamics: Application to clinical ECG with ventricular tachycardia. IEEE Trans. Biomed. Eng. **59**(8), 2111–7 (2012)
41. Cherry, E., Fenton, F.: Suppression of alternans and conduction blocks despite steep apd restitution: electrotonic, memory, and conduction velocity restitution effects. Am J Physiol. Heart Circ. Physiol. **286**(6), H2332–2341 (2004)
42. Constantino, J., Long, Y., Ashihara, T., Trayanova, N.A.: Tunnel propagation following defibrillation with icd shocks: hidden postshock activations in the left ventricular wall underlie isoelectric window. Heart Rhythm **7**(7), 953–61 (2010)
43. Courtemanche, M., Ramirez, R.J., Nattel, S.: Ionic mechanisms underlying human atrial action potential properties: insights from a mathematical model. Am. J. Physiol. **275**(1 Pt 2), H301–21 (1998)
44. Deo, M., Boyle, P., Plank, G., Vigmond, E.: Arrhythmogenic mechanisms of the Purkinje system during electric shocks: a modeling study. Heart Rhythm **6**(12), 1782–9 (2009)

45. Deo, M., Boyle, P.M., Kim, A.M., Vigmond, E.J.: Arrhythmogenesis by single ectopic beats originating in the Purkinje system. Am. J. Physiol. Heart Circ. Physiol. **299**(4), H1002–11 (2010)
46. Deo, M., Ruan, Y., Pandit, S.V., Shah, K., Berenfeld, O., Blaufox, A., Cerrone, M., Noujaim, S.F., Denegri, M., Jalife, J., Priori, S.G.: KCNJ2 mutation in short QT syndrome 3 results in atrial fibrillation and ventricular proarrhythmia. Proc. Natl. Acad. Sci. USA **110**(11), 4291–6 (2013)
47. Doshi, A.N., Idriss, S.F.: Effect of resistive barrier location on the relationship between t-wave alternans and cellular repolarization alternans: a 1-D modeling study. J. Electrocardiol. **43**(6), 566–71 (2010)
48. Dux-Santoy, L., Sebastian, R., Felix-Rodriguez, J., Ferrero, J.M., Saiz, J.: Interaction of specialized cardiac conduction system with antiarrhythmic drugs: a simulation study. IEEE Trans. Biomed. Eng. **58**(12), 3475–8 (2011)
49. Entcheva, E.: Cardiac optogenetics. Am. J. Physiol. Heart Circ. Physiol. **304**(9), H1179–91 (2013)
50. Entcheva, E., Trayanova, N.A., Claydon, F.J.: Patterns of and mechanisms for shock-induced polarization in the heart: a bidomain analysis. IEEE Trans. Biomed. Eng. **46**(3), 260–70 (1999)
51. Fenton, F.H., Cherry, E.M., Hastings, H.M., Evans, S.J.: Multiple mechanisms of spiral wave breakup in a model of cardiac electrical activity. Chaos **12**(3), 852–892 (2002)
52. Fink, M., Niederer, S.A., Cherry, E.M., Fenton, F.H., Koivumaki, J.T., Seemann, G., Thul, R., Zhang, H., Sachse, F.B., Beard, D., Crampin, E.J., Smith, N.P.: Cardiac cell modelling: Observations from the heart of the cardiac physiome project. Progress in Biophysics & Molecular Biology **104**(1–3), 2–21 (2011)
53. Fink, M., Noble, D., Virag, L., Varro, A., Giles, W.R.: Contributions of hERG K+ current to repolarization of the human ventricular action potential. Prog. Biophys. Mol. Biol. **96**(1-3), 357–76 (2008)
54. Garfinkel, A., Kim, Y.H., Voroshilovsky, O., Qu, Z., Kil, J.R., Lee, M.H., Karagueuzian, H.S., Weiss, J.N., Chen, P.S.: Preventing ventricular fibrillation by flattening cardiac restitution. Proc. Natl. Acad. Sci. USA **97**(11), 6061–6 (2000)
55. Goldberger, J.J., Buxton, A.E., Cain, M., Costantini, O., Exner, D.V., Knight, B.P., Lloyd-Jones, D., Kadish, A.H., Lee, B., Moss, A., Myerburg, R., Olgin, J., Passman, R., Rosenbaum, D., Stevenson, W., Zareba, W., Zipes, D.P.: Risk stratification for arrhythmic sudden cardiac death: identifying the roadblocks. Circulation **123**(21), 2423–30 (2011)
56. Grandi, E., Pandit, S.V., Voigt, N., Workman, A.J., Dobrev, D., Jalife, J., Bers, D.M.: Human atrial action potential and Ca2+ model: sinus rhythm and chronic atrial fibrillation. Circ. Res. **109**(9), 1055–66 (2011)
57. Grandi, E., Pasqualini, F.S., Bers, D.M.: A novel computational model of the human ventricular action potential and Ca transient. J Mol Cell Cardiol **48**(1), 112–21 (2010)
58. Hohnloser, S.H., Ikeda, T., Cohen, R.J.: Evidence regarding clinical use of microvolt t-wave alternans. Heart Rhythm **6**(3 Suppl), S36–44 (2009)
59. Hoogendijk, M.G., Potse, M., Vinet, A., de Bakker, J.M., Coronel, R.: ST segment elevation by current-to-load mismatch: an experimental and computational study. Heart Rhythm **8**(1), 111–8 (2011)
60. Hu, Y., Gurev, V., Constantino, J., Bayer, J.D., Trayanova, N.A.: Effects of mechano-electric feedback on scroll wave stability in human ventricular fibrillation. PLoS. One. **8**(4), e60,287 (2013)

61. Ijiri, T., Ashihara, T., Yamaguchi, T., Takayama, K., Igarashi, T., Shimada, T., Namba, T., Haraguchi, R., Nakazawa, K.: A procedural method for modeling the Purkinje fibers of the heart. J. Physiol. Sci. **58**(7), 481–6 (2008)
62. Jessup, M., Greenberg, B., Mancini, D., Cappola, T., Pauly, D.F., Jaski, B., Yaroshinsky, A., Zsebo, K.M., Dittrich, H., Hajjar, R.J., Calcium Upregulation by Percutaneous Administration of Gene Therapy in Cardiac Disease, I.: Calcium upregulation by percutaneous administration of gene therapy in cardiac disease (CUPID): a phase 2 trial of intracoronary gene therapy of sarcoplasmic reticulum Ca2+-ATPase in patients with advanced heart failure. Circulation **124**(3), 304–13 (2011)
63. Jie, X., Gurev, V., Trayanova, N.: Mechanisms of mechanically induced spontaneous arrhythmias in acute regional ischemia. Circ. Res. **106**(1), 185–92 (2010)
64. Jie, X., Rodriguez, B., de Groot, J.R., Coronel, R., Trayanova, N.: Reentry in survived subepicardium coupled to depolarized and inexcitable midmyocardium: insights into arrhythmogenesis in ischemia phase 1b. Heart Rhythm **5**(7), 1036–44 (2008)
65. Jie, X., Trayanova, N.A.: Mechanisms for initiation of reentry in acute regional ischemia phase 1b. Heart Rhythm **7**(3), 379–86 (2010)
66. Jons, C., O-Uchi, J., Moss, A.J., Reumann, M., Rice, J.J., Goldenberg, I., Zareba, W., Wilde, A.A., Shimizu, W., Kanters, J.K., McNitt, S., Hofman, N., Robinson, J.L., Lopes, C.M.: Use of mutant-specific ion channel characteristics for risk stratification of long QT syndrome patients. Sci. Transl. Med. **3**(76), 76ra28 (2011)
67. Keldermann, R.H., Nash, M.P., Gelderblom, H., Wang, V.Y., Panfilov, A.V.: Electromechanical wavebreak in a model of the human left ventricle. Am. J. Physiol. Heart Circ. Physiol. **299**(1), H134–43 (2010)
68. Keldermann, R.H., ten Tusscher, K.H., Nash, M.P., Bradley, C.P., Hren, R., Taggart, P., Panfilov, A.V.: A computational study of mother rotor VF in the human ventricles. Am. J. Physiol. Heart Circ. Physiol. **296**(2), H370–9 (2009)
69. Keldermann, R.H., ten Tusscher, K.H., Nash, M.P., Hren, R., Taggart, P., Panfilov, A.V.: Effect of heterogeneous apd restitution on VF organization in a model of the human ventricles. Am. J. Physiol. Heart Circ. Physiol. **294**(2), H764–74 (2008)
70. Kim, R.H., Kim, D.H., Xiao, J., Kim, B.H., Park, S.I., Panilaitis, B., Ghaffari, R., Yao, J., Li, M., Liu, Z., Malyarchuk, V., Kim, D.G., Le, A.P., Nuzzo, R.G., Kaplan, D.L., Omenetto, F.G., Huang, Y., Kang, Z., Rogers, J.A.: Waterproof AlInGaP optoelectronics on stretchable substrates with applications in biomedicine and robotics. Nat. Mater. **9**(11), 929–37 (2010)
71. Li, P., Rudy, Y.: A model of canine purkinje cell electrophysiology and Ca(2+) cycling: rate dependence, triggered activity, and comparison to ventricular myocytes. Circ. Res. **109**(1), 71–9 (2011)
72. Li, W., Gurev, V., McCulloch, A.D., Trayanova, N.A.: The role of mechanoelectric feedback in vulnerability to electric shock. Prog. Biophys. Mol. Biol. **97**(2-3), 461–78 (2008)
73. Li, W., Janardhan, A.H., Fedorov, V.V., Sha, Q., Schuessler, R.B., Efimov, I.R.: Low-energy multistage atrial defibrillation therapy terminates atrial fibrillation with less energy than a single shock. Circ. Arrhythm. Electrophysiol. **4**(6), 917–25 (2011)
74. Li, W., Kohl, P., Trayanova, N.: Induction of ventricular arrhythmias following mechanical impact: a simulation study in 3D. J. Mol. Histol. **35**(7), 679–86 (2004)
75. Li, W., Kohl, P., Trayanova, N.: Myocardial ischemia lowers precordial thump efficacy: an inquiry into mechanisms using three-dimensional simulations. Heart Rhythm **3**(2), 179–86 (2006)

76. Li, W., Ripplinger, C.M., Lou, Q., Efimov, I.R.: Multiple monophasic shocks improve electrotherapy of ventricular tachycardia in a rabbit model of chronic infarction. Heart Rhythm **6**(7), 1020–7 (2009)
77. Lin, J.Y., Knutsen, P.M., Muller, A., Kleinfeld, D., Tsien, R.Y.: ReaChR: a red-shifted variant of channelrhodopsin enables deep transcranial optogenetic excitation. Nat. Neurosci. **16**(10), 1499–508 (2013)
78. Lindblom, A.E., Roth, B.J., Trayanova, N.A.: Role of virtual electrodes in arrhythmogenesis: pinwheel experiment revisited. J. Cardiovasc. Electrophysiol. **11**(3), 274–85 (2000)
79. Luther, S., Fenton, F.H., Kornreich, B.G., Squires, A., Bittihn, P., Hornung, D., Zabel, M., Flanders, J., Gladuli, A., Campoy, L., Cherry, E.M., Luther, G., Hasenfuss, G., Krinsky, V.I., Pumir, A., Gilmour R. F., J., Bodenschatz, E.: Low-energy control of electrical turbulence in the heart. Nature **475**(7355), 235–9 (2011)
80. Merchant, F.M., Armoundas, A.A.: Role of substrate and triggers in the genesis of cardiac alternans, from the myocyte to the whole heart: implications for therapy. Circulation **125**(3), 539–49 (2012)
81. Meunier, J.M., Eason, J.C., Trayanova, N.A.: Termination of reentry by a long-lasting ac shock in a slice of canine heart: a computational study. J. Cardiovasc. Electrophysiol. **13**(12), 1253–61 (2002)
82. Meunier, J.M., Trayanova, N.A., Gray, R.A.: Sinusoidal stimulation of myocardial tissue: effects on single cells. J. Cardiovasc. Electrophysiol. **10**(12), 1619–30 (1999)
83. Meunier, J.M., Trayanova, N.A., Gray, R.A.: Entrainment by an extracellular AC stimulus in a computational model of cardiac tissue. J. Cardiovasc. Electrophysiol. **12**(10), 1176–84 (2001)
84. Moreno, J.D., Zhu, Z.I., Yang, P.C., Bankston, J.R., Jeng, M.T., Kang, C., Wang, L., Bayer, J.D., Christini, D.J., Trayanova, N.A., Ripplinger, C.M., Kass, R.S., Clancy, C.E.: A computational model to predict the effects of class I anti-arrhythmic drugs on ventricular rhythms. Sci. Transl. Med. **3**(98), 98ra83 (2011)
85. Narayan, S.M., Bayer, J.D., Lalani, G., Trayanova, N.A.: Action potential dynamics explain arrhythmic vulnerability in human heart failure: a clinical and modeling study implicating abnormal calcium handling. J. Am. Coll. Cardiol. **52**(22), 1782–92 (2008)
86. Narayan, S.M., Franz, M.R., Lalani, G., Kim, J., Sastry, A.: T-wave alternans, restitution of human action potential duration, and outcome. J. Am. Coll. Cardiol. **50**(25), 2385–92 (2007)
87. Ng, J., Jacobson, J.T., Ng, J.K., Gordon, D., Lee, D.C., Carr, J.C., Goldberger, J.J.: Virtual electrophysiological study in a 3-dimensional cardiac magnetic resonance imaging model of porcine myocardial infarction. J. Am. Coll. Cardiol. **60**(5), 423–30 (2012)
88. Noble, D.: Modeling the heart–from genes to cells to the whole organ. Science **295**(5560), 1678–1682 (2002)
89. Nygren, A., Fiset, C., Firek, L., Clark, J.W., Lindblad, D.S., Clark, R.B., Giles, W.R.: Mathematical model of an adult human atrial cell: the role of K+ currents in repolarization. Circ. Res. **82**(1), 63–81 (1998)
90. O'Hara, T., Rudy, Y.: Arrhythmia formation in subclinical ("silent") long QT syndrome requires multiple insults: Quantitative mechanistic study using the KCNQ1 mutation q357r as example. Heart Rhythm **9**(2), 275–82 (2012)
91. O'Hara, T., Virag, L., Varro, A., Rudy, Y.: Simulation of the undiseased human cardiac ventricular action potential: model formulation and experimental validation. PLoS. Comput. Biol. **7**(5), e1002,061 (2011)
92. Pandit, S.V., Jalife, J.: Rotors and the dynamics of cardiac fibrillation. Circ. Res. **112**(5), 849–62 (2013)

93. Plonsey, R., Barr, R.C.: Bioelectricity : a quantitative approach, 3rd edn. Springer, New York, NY (2007)
94. Pop, M., Sermesant, M., Mansi, T., Crystal, E., Ghate, S., Peyrat, J., Lashevsky, I., Beiping, Q., McVeigh, E., Ayache, N., Wright, G.A.: Correspondence between simple 3-D MRI-based computer models and in-vivo ep measurements in swine with chronic infarctions. IEEE Trans. Biomed. Eng. **58**(12), 3483–6 (2011)
95. Potse, M., Krause, D., Bacharova, L., Krause, R., Prinzen, F.W., Auricchio, A.: Similarities and differences between electrocardiogram signs of left bundle-branch block and left-ventricular uncoupling. Europace **14**(Suppl 5), v33–v39 (2012)
96. Rantner, L.J., Arevalo, H.J., Constantino, J.L., Efimov, I.R., Plank, G., Trayanova, N.A.: Three-dimensional mechanisms of increased vulnerability to electric shocks in myocardial infarction: Altered virtual electrode polarizations and conduction delay in the peri-infarct zone. J. Physiol. **590**(Pt 18), 4537–4551 (2012)
97. Rantner, L.J., Tice, B.M., Trayanova, N.A.: Terminating ventricular tachyarrhythmias using far-field low-voltage stimuli: Mechanisms and delivery protocols. Heart Rhythm **10**(8), 1209–17 (2013)
98. Rantner, L.J., Vadakkumpadan, F., Spevak, P.J., Crosson, J.E., Trayanova, N.A.: Placement of implantable cardioverter-defibrillators in paediatric and congenital heart defect patients: A pipeline for model generation and simulation prediction of optimal configurations. J. Physiol. **591**, 4321–34 (2013)
99. Relan, J., Chinchapatnam, P., Sermesant, M., Rhode, K., Ginks, M., Delingette, H., Rinaldi, C.A., Razavi, R., Ayache, N.: Coupled personalization of cardiac electrophysiology models for prediction of ischaemic ventricular tachycardia. Interface Focus **1**(3), 396–407 (2011)
100. Richards, D.F., Glosli, J.N., Draeger, E.W., Mirin, A.A., Chan, B., Fattebert, J.L., Krauss, W.D., Oppelstrup, T., Butler, C.J., Gunnels, J.A., Gurev, V., Kim, C., Magerlein, J., Reumann, M., Wen, H.F., Rice, J.J.: Towards real-time simulation of cardiac electrophysiology in a human heart at high resolution. Comput. Methods Biomech. Biomed. Engin. **16**(7), 802–5 (2013)
101. Roberts, B.N., Yang, P.C., Behrens, S.B., Moreno, J.D., Clancy, C.E.: Computational approaches to understand cardiac electrophysiology and arrhythmias. Am. J. Physiol. Heart Circ. Physiol. **303**(7), H766–H783 (2012)
102. Robichaux, R.P., Dosdall, D.J., Osorio, J., Garner, N.W., Li, L., Huang, J., Ideker, R.E.: Periods of highly synchronous, non-reentrant endocardial activation cycles occur during long-duration ventricular fibrillation. J. Cardiovasc. Electrophysiol **21**(11), 1266–73 (2010)
103. Rodriguez, B., Eason, J.C., Trayanova, N.: Differences between left and right ventricular anatomy determine the types of reentrant circuits induced by an external electric shock. a rabbit heart simulation study. Prog Biophys Mol Biol **90**(1-3), 399–413 (2006)
104. Rodriguez, B., Li, L., Eason, J.C., Efimov, I.R., Trayanova, N.A.: Differences between left and right ventricular chamber geometry affect cardiac vulnerability to electric shocks. Circ. Res. **97**(2), 168–75 (2005)
105. Rodriguez, B., Tice, B.M., Eason, J.C., Aguel, F., Ferrero J. M., J., Trayanova, N.: Effect of acute global ischemia on the upper limit of vulnerability: a simulation study. Am. J. Physiol. Heart Circ. Physiol. **286**(6), H2078–88 (2004)
106. Rodriguez, B., Tice, B.M., Eason, J.C., Aguel, F., Trayanova, N.: Cardiac vulnerability to electric shocks during phase 1a of acute global ischemia. Heart Rhythm **1**(6), 695–703 (2004)

107. Rodriguez, B., Trayanova, N.: Upper limit of vulnerability in a defibrillation model of the rabbit ventricles. J. Electrocardiol. **36**(Suppl.), 51–6 (2003)
108. Sampson, K.J., Iyer, V., Marks, A.R., Kass, R.S.: A computational model of Purkinje fibre single cell electrophysiology: implications for the long QT syndrome. J. Physiol. **588**(Pt 14), 2643–55 (2010)
109. Sebastian, R., Zimmerman, V., Romero, D., Sanchez-Quintana, D., Frangi, A.F.: Characterization and modeling of the peripheral cardiac conduction system. IEEE Trans. Med. Imaging **32**(1), 45–55 (2013)
110. Spiteri, R.J., Dean, R.C.: Stiffness analysis of cardiac electrophysiological models. Ann. Biomed. Eng. **38**(12), 3592–604 (2010)
111. Stevenson, W.G., Brugada, P., Waldecker, B., Zehender, M., Wellens, H.J.: Clinical, angiographic, and electrophysiologic findings in patients with aborted sudden death as compared with patients with sustained ventricular tachycardia after myocardial infarction. Circulation **71**(6), 1146–52 (1985)
112. Stewart, P., Aslanidi, O.V., Noble, D., Noble, P.J., Boyett, M.R., Zhang, H.: Mathematical models of the electrical action potential of Purkinje fibre cells. Philos. Trans. A Math. Phys. Eng. Sci. **367**(1896), 2225–55 (2009)
113. Tandri, H., Weinberg, S.H., Chang, K.C., Zhu, R., Trayanova, N.A., Tung, L., Berger, R.D.: Reversible cardiac conduction block and defibrillation with high-frequency electric field. Sci. Transl. Med. **3**(102), 102ra96 (2011)
114. Ten Tusscher, K.H., Hren, R., Panfilov, A.V.: Organization of ventricular fibrillation in the human heart. Circ. Res. **100**(12), e87–101 (2007)
115. Trayanova, N., Constantino, J., Ashihara, T., Plank, G.: Modeling defibrillation of the heart: approaches and insights. IEEE Rev Biomed Eng **4**, 89–102 (2011)
116. Trayanova, N., Eason, J., Aguel, F.: Cardiac defibrillation: A look inside the heart. Computing and Visualization in Science **3**, 259–270 (2002)
117. Trayanova, N., Li, W., Eason, J., Kohl, P.: Effect of stretch-activated channels on defibrillation efficacy. Heart Rhythm **1**(1), 67–77 (2004)
118. Trayanova, N., Skouibine, K., Moore, P.: Virtual electrode effects in defibrillation. Prog. Biophys. Mol. Biol. **69**(2-3), 387–403 (1998)
119. Trayanova, N.A.: Whole-heart modeling: applications to cardiac electrophysiology and electromechanics. Circ. Res. **108**(1), 113–28 (2011)
120. Trayanova, N.A., Gurev, V., Constantino, J., Hu, Y.: Mathematical models of ventricular mechano-electric coupling and arrhythmia, 2nd edn., pp. 258–268. Oxford University Press, Oxford, New York (2011)
121. ten Tusscher, K.H., Panfilov, A.V.: Alternans and spiral breakup in a human ventricular tissue model. Am. J. Physiol. Heart Circ. Physiol. **291**(3), H1088–100 (2006)
122. Vadakkumpadan, F., Arevalo, H., Ceritoglu, C., Miller, M., Trayanova, N.: Image-based estimation of ventricular fiber orientations for personalized modeling of cardiac electrophysiology. IEEE Trans. Med. Imaging **31**(5), 1051–60 (2012)
123. Vadakkumpadan, F., Arevalo, H., Prassl, A.J., Chen, J., Kickinger, F., Kohl, P., Plank, G., Trayanova, N.: Image-based models of cardiac structure in health and disease. Wiley Interdiscip. Rev. Syst. Biol. Med. **2**(4), 489–506 (2010)
124. Vaidyanathan, R., O'Connell, R.P., Deo, M., Milstein, M.L., Furspan, P., Herron, T.J., Pandit, S.V., Musa, H., Berenfeld, O., Jalife, J., Anumonwo, J.M.: The ionic bases of the action potential in isolated mouse cardiac Purkinje cell. Heart Rhythm **10**(1), 80–7 (2013)

125. Veenhuyzen, G.D., Coverett, K., Quinn, F.R., Sapp, J.L., Gillis, A.M., Sheldon, R., Exner, D.V., Mitchell, L.B.: Single diagnostic pacing maneuver for supraventricular tachycardia. Heart Rhythm **5**(8), 1152–8 (2008)
126. Vigmond, E., Vadakkumpadan, F., Gurev, V., Arevalo, H., Deo, M., Plank, G., Trayanova, N.: Towards predictive modelling of the electrophysiology of the heart. Exp. Physiol. **94**(5), 563–77 (2009)
127. Wang, L., Wong, K.C., Zhang, H., Liu, H., Shi, P.: Noninvasive computational imaging of cardiac electrophysiology for 3-D infarct. IEEE Trans. Biomed. Eng. **58**(4), 1033–43 (2011)
128. Weinberg, S.H., Chang, K.C., Zhu, R., Tandri, H., Berger, R.D., Trayanova, N.A., Tung, L.: Defibrillation success with high frequency electric fields is related to degree and location of conduction block. Heart Rhythm **10**(5), 740–8 (2013)
129. Weiss, J.N., Nivala, M., Garfinkel, A., Qu, Z.: Alternans and arrhythmias: from cell to heart. Circ. Res. **108**(1), 98–112 (2011)
130. Wilhelms, M., Rombach, C., Scholz, E.P., Dossel, O., Seemann, G.: Impact of amiodarone and cisapride on simulated human ventricular electrophysiology and electrocardiograms. Europace **14**(Suppl 5), v90–v96 (2012)
131. Williams, J.C., Xu, J., Lu, Z., Klimas, A., Chen, X., Ambrosi, C.M., Cohen, I.S., Entcheva, E.: Computational optogenetics: empirically-derived voltage- and light-sensitive channelrhodopsin-2 model. PLoS. Comput. Biol. **9**(9), e1003,220 (2013)
132. Winslow, R.L., Trayanova, N., Geman, D., Miller, M.I.: Computational medicine: translating models to clinical care. Sci. Transl. Med. **4**(158), 158rv11 (2012)
133. Wong, J., Abilez, O.J., Kuhl, E.: Computational optogenetics: A novel continuum framework for the photoelectrochemistry of living systems. J. Mech. Phys. Solids **60**(6), 1158–1178 (2012)
134. Xia, L., Zhang, Y., Zhang, H., Wei, Q., Liu, F., Crozier, S.: Simulation of Brugada syndrome using cellular and three-dimensional whole-heart modeling approaches. Physiol. Meas.**27**(11), 1125–42 (2006)
135. Yang, F.: Simulation of electrocardiographic manifestation of healed infarctions using a 3D realistic rabbit ventricular model. Int. J. Cardiol. **152**(1), 121–3 (2011)
136. Zemzemi, N., Bernabeu, M.O., Saiz, J., Cooper, J., Pathmanathan, P., Mirams, G.R., Pitt-Francis, J., Rodriguez, B.: Computational assessment of drug-induced effects on the electrocardiogram: from ion channel to body surface potentials. Br. J. Pharmacol. **168**(3), 718–33 (2013)
137. Zhao, J.T., Hill, A.P., Varghese, A., Cooper, A.A., Swan, H., Laitinen-Forsblom, P.J., Rees, M.I., Skinner, J.R., Campbell, T.J., Vandenberg, J.I.: Not all hERG pore domain mutations have a severe phenotype: g584s has an inactivation gating defect with mild phenotype compared to g572s, which has a dominant negative trafficking defect and a severe phenotype. J. Cardiovasc. Electrophysiol. **20**(8), 923–30 (2009)
138. Zhu, X., Wei, D., Okazaki, O.: Computer simulation of clinical electrophysiological study. Pacing Clin. Electrophysiol. **35**(6), 718–29 (2012)